Journal of Applied Sciences

ISSN 1812-5654

science alert

ANSInet
an open access publisher
http://ansinet.com

Journal of Applied Sciences 13 (15): 3042-3048, 2013
ISSN 1812-5654 / DOI: 10.3923/jas.2013.3042.3048

Research on the Aeroelastic Response of Tower Effects for Great Grade Wind Turbine

Pinting Zhang, Shuhong Huang, Tao Yang and Jianlan Li
School of Energy and Power Engineering, Huazhong University of Science and Technology, Wuhan, 430074, China

Abstract: With the increasing size of wind turbines, the rotor-tower interference cannot be neglected. Based on potential flow method, flow field around the tower was simulated and compared to CFD method. The quasi-steady aeroelastic model under tower interference was established and the code was developed. Taking NREL-5MW Reference Wind Turbine as an example, the output power of rotor and the loads of the blades were calculated during tower passage. Results showed that tower interference had little effect on average output power whereas it greatly affected the instant output power and it led great impulsive aerodynamic load at azimuth angle of 180 degree. To flexible blades, the fluctuation of power and the loads of blades were bigger than rigid blades. Then, different wind rotors with shorter or longer main shafts were simulated under tower interference and the rotors with shorter shafts experienced bigger fluctuation. The limiting position calculations of flexible blades under wind trust force showed that the blades of rotors with too short shafts had to dare the risk of crashing into tower.

Key words: Wind turbine, tower interference, aeroelasticity, short shaft turbine

INTRODUCTION

During the revolution, wind field seen by rotor is influenced by the interaction with tower. With the up-scaling trend of the wind turbine, the influence of rotor-tower interaction become more significant when analyzed in a more flexible and lower stiffness wind rotor (Kong *et al*., 2011). To an upwind turbine, the tower-rotor interaction is mainly caused by obstruction when the free flow past the tower, which means the periodic experienced wind speed decreasing during revolution (Hasegawa *et al*., 2006). To upwind rotor, potential flow method can provide the quasi-steady wind speed model around the tower. Zahle *et al*. (2008) simulated the steady loads to the NREL-5MW Reference Wind Turbine (NREL-5MW RWT) with rigid blades using Computed Fluid Dynamic (CFD) methods (EllipSys3D) and compared with the results of HAWC2, which using a potential flow wind speed model and Blade Element Momentum (BEM) method. The results both showed the periodic and impulsive load when the blades past the tower but HAWC2 appeared to consistently over predict the tower shadow compared to the EllipSys3D results by as much as 100% on both the thrust and the torque. Then Zahle *et al*. (2009) simulated the unsteady load to a typical blade section during tower passage by 2D CFD method and compared with HAWC2 and experiments. The comparison showed that the potential flow method basically predicted rotor-tower interaction wind speed model but HAWC2 might over predict the influence of the tower interference.

With the increasing size of the modern wind turbine, the blades of the rotor became more flexible. When the flexible rotors experience the periodic and impulsive aerodynamic loads during tower passage, the dynamic vibration response of the blades will be feedback to the aerodynamic loads, hence, the problem of vibration and aeroelastic stability of wind rotor are compounded by the impulsive and periodic wind speed due to tower interference (Hansen *et al*., 2006). In order to reduce the weight of the nacelle therefore pursue higher economic returns, a compact structure with shorter main shaft is often adopted in modern wind turbine and leads more severe tower interference effect.

In this study, taking the NREL-5MW RWT as an example, a 3D potential flow method wind speed model was introduced and the aeroelastic response of upwind rotor during tower passage was studied. Then the basic principle of aeroelastic response to tower interference for wind rotors with various main shafts in length was studied.

Corresponding Author: Tao Yang, School of Energy and Power Engineering, Huazhong University of Science and Technology, Wuhan, 430074, China

MODELS

Coordinate system: The wind flow field and the vibration of the wind rotor are described by four coordinate systems shown in Fig. 1. First, an inertial system (coordinate system 1) is placed at the bottom of the tower. System 2 is non-rotating and placed in the nacelle, system 3 is fixed to the rotating shaft and system 4 is aligned with one of the blades.

3D potential wind speed model and aerodynamic model: Lackner *et al.* (2013) general semi-infinite line of 3D doublets with vary strength was adopted to substitute the tower in this paper, as Eq. 1.

$$\phi_{3d} = \int_{-\infty}^{H} \frac{\mu(x_0)}{4\pi} \frac{z}{\left[(x-x_0)^2 + y^2 + z^2\right]^{3/2}} dx_0 \quad (1)$$

Here, the $\mu(x_0)$ varies form $x_0 = H$ to $x_0 = -\infty$. The gradient of ϕ_{3d}, as Eq. 3, yields the inducing velocity components and the no-entry boundary condition on the tower surface is used to solve for the strength distribution of the doublets. It is clearly that x_0 cannot extend to $-\phi$-∞ and in this study, a value of ten times of the tower height are used to guarantee the convergence. In coordinate system 1, x and μ was discrete to $x_1 \ldots x_n$ and $\mu_1 \ldots \mu_n$ equally and the $\mu(x_0)$ can be numerically solved by Eq. 2:

$$\begin{bmatrix} f(1,1)\cdot dx_0 & \cdots & f(1,n)\cdot dx_0 \\ \vdots & \ddots & \vdots \\ f(n,1)\cdot dx_0 & \cdots & f(n,n)\cdot dx_0 \end{bmatrix} \begin{Bmatrix} \mu_1 \\ \vdots \\ \mu_n \end{Bmatrix} = -\begin{Bmatrix} U_\infty(x_1) \\ \vdots \\ U_\infty(x_n) \end{Bmatrix} \quad (2)$$

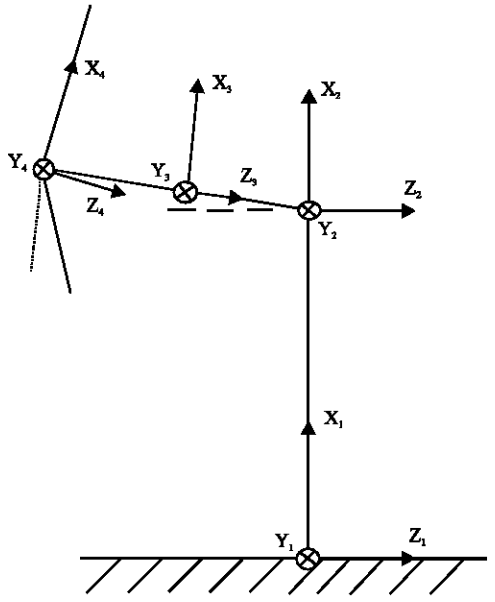

Fig. 1: Coordinate systems for wind turbine

Here:

$$\int_{-\infty}^{H} f(i,j)\,dx_0 = \int_{-\infty}^{H} f\left((x_i, y, z), x_j\right) dx_0 = \frac{\partial \phi_{3d}}{\partial x}$$

$$u = \frac{\partial \phi_{3d}}{\partial x},\ v = \frac{\partial \phi_{3d}}{\partial y},\ w = \frac{\partial \phi_{3d}}{\partial z} \quad (3)$$

Here, u, v, w are the inducing velocity and the wind speed seen by blades in coordinate system 1 can be calculated by Eq. 4:

$$V_x = u, V_y = v, V_z = w + V_\infty \quad (4)$$

To NREL-5MW RWT, the height of tower H = 90, with the radius of R (H) = 1.935 m (at top) and radius of R (0) = 3 m (at bottom), the rated speed at hub $V\infty$ = 11.4 (Jonkman *et al.*, 2009). The experiencing wind speed of blade tip during revolution in coordinate system 1 was calculated by Eq. 4 and compared with the CFD inviscid method, as shown in Fig. 2. The result showed little difference and clearly showed the impulsive load during tower passage. Due to the obstruction of the tower, flow in both sides of the tower were opposite in direction Y and the wind speed in tower interference zone was a little higher than rated wind speed in direction Z.

Blade Element Momentum (BEM) method with Prantdl's tip loss model (Hansen, 2008) was used to calculate the aerodynamic of the rotor. According to NREL-5MW RWT, the blade was discrete to 17 strips and the aerodynamic parameters of each strip can obtained from Jonkman *et al.* (2009).

Structural dynamic model: In this study, the blade is treated as 1D equivalent beam and the FEM method is used to solve the structural dynamics of the blade. According to Jonkman and Butterfield (2009), each blade is discrete to 48 beam elements and the whole rotor is discrete to 144 beam elements and 145 nodes. Each node has 6 degrees of freedom (DOFs) and the total number of DOFs of whole rotor is 870. The structural dynamic of the wind rotor can be described by Eq. 5.

$$M\ddot{x} + C\dot{x} + Kx = F \quad (5)$$

where, the M, C, K are the mass matrix, damping matrix and stiffness matrix respectively, with size of 870*870 and $\ddot{x}, \dot{x}, x$ are vectors represented the acceleration, velocity and displacement of DOFs. F includes the aerodynamic load which can be calculated by BEM method, centrifugal load and gravity load. Then a 4 order Runger Kutta method is used and a matlab code is developed to solve Eq. 5.

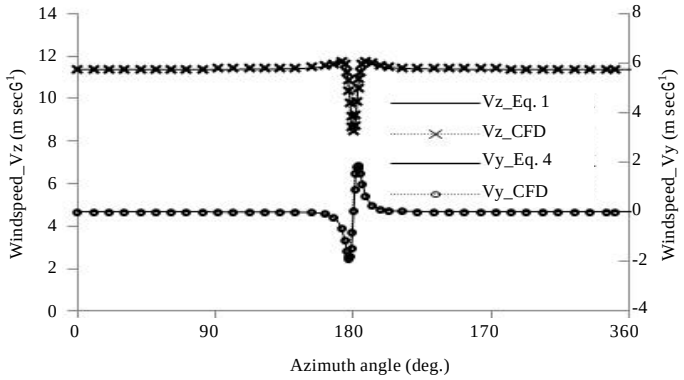

Fig. 2: Wind speed distribution of a distance of 5 m from tower center

Coupling model: The coupling between structural dynamic and aerodynamic includes the experienced wind speed change due to edgewise and flapwise vibration of the blade and the Angle of Attack (AOA) change due to torsional vibration. The wind rotor is assumed to be completely opposite to flow, which means that the yaw degree angle equals zero, the wind speed seen by the rotor during revolution can be calculated by Eq. 4 and 6:

$$\begin{cases} V_{rel,y} = V_y + v_{b,y} \\ V_{rel,z} = V_z + v_{b,z} \end{cases} \quad (6)$$

where, $v_{b,y}$ and $v_{b,z}$ are the vibration velocity of the each strip and can be obtained from Eq. 5.

The real AOA of the blade can be calculated by Eq. 7:

$$\alpha_{rel} = \varphi - (\beta + \theta_p) + \alpha_{b,v} \quad (7)$$

where, $\alpha_{b,v}$ is the torsional vibration of the blade and can be calculated by Eq. 5. φ is the angle between the real wind seen by blade and the wind rotor plane, $(\beta+\theta_p)$ is the summary of installation angle and pitch angle.

Because the structural element node and strip node do not one-to-one correspond, Chebyshev Interpolation is used to get the strip vibration velocity. In each step time, the aerodynamic load is calculated by BEM method and then the structural dynamic response of the wind rotor, which is the input of the Eq. 6 and 7 in next step time, can be calculated by Eq. 5. Then the aeroelastic response of the rotor can be calculated. The flow chart of the simulation is shown in Fig. 3.

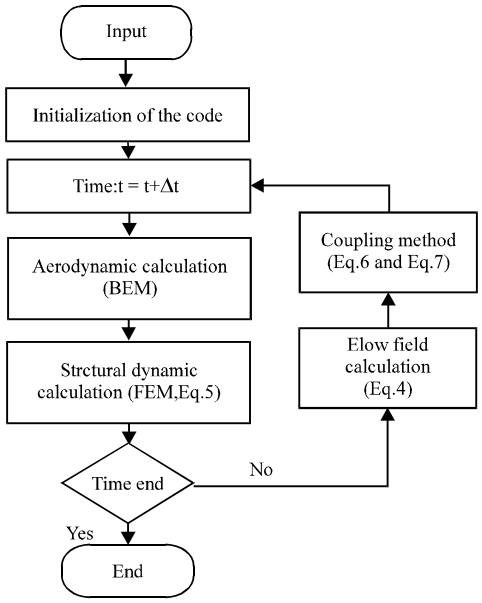

Fig. 3: Flow chart of aeroelastic simulation

RESULTS AND DISCUSSION

Response of the rigid rotor to tower interference: BEM method with Prantdl's tip loss model was used to calculate the aerodynamic of NREL-5MW RWT. The output power of the rigid rotor under uniform wind was 5.32MW, which was little higher than the rated power given in Jonkman and Butterfield (2009). Then the response of the rigid rotor to tower interference was calculated, the results were shown in Fig. 4-6.

The obstruction to the flow by tower changed the wind speed and the direction of the flow. Figure 4 and 5 showed that the blades experienced slightly higher load

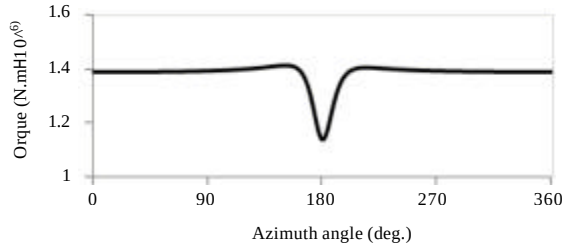

Fig. 4: Shaft torque of rotor with rigid blades

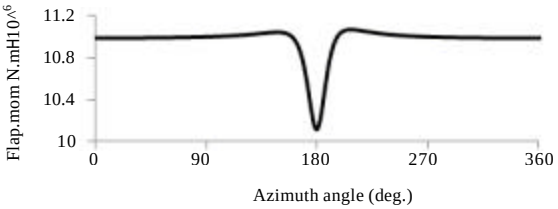

Fig. 5: Flapwise moment of rigid blades

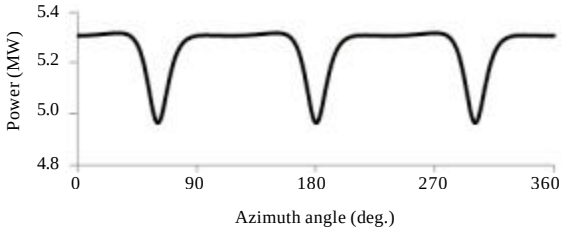

Fig. 6: Output power of rotor with rigid blades

when the blades entranced the tower interference zone, then the load of the rotor dramatically decreased near the azimuth angle of 180° (when the blade at top of the rotor, the azimuth was defined as 0 degree). When leaving the tower interference zone, the load of the rotor recoveried fast. Compared with the rotor in uniform flow, at azimuth degree of 180°, the main shaft torque, Fig. 4, showed an approximate 17.9% reduction and deflection moment of blade root, Fig. 5, showed an approximate 7.8% reduction. Due to the experiencing opposite flow in direction Y, the main shaft torque and flapwise moment of blade showed a certain asymmetry. According to the direction of rotation, the main shaft torque when blades entranced the tower shadow zone was slightly bigger, while the blade deflection moment is slightly smaller than the loads when blades left the tower shadow zone. The maximum value of main shaft torque and blade deflection moment showed 2.1 and 0.8% increment, respectively. Figure 5 is the output power of the rotor during revolution which showed an obvious 3P fluctuation of load. The average output power showed a very slightly reduction of 0.3%

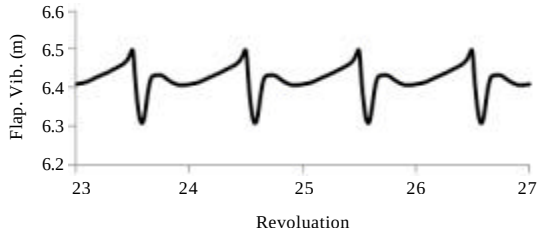

Fig. 7: Flap vibration of blade tip during revolution (in coordinate 4)

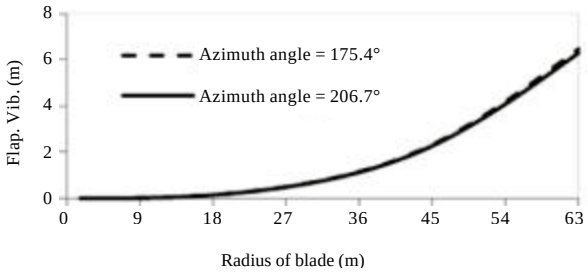

Fig. 8: Limiting position of blade of flap vibration during revolution (in coordinate 4)

output power in uniform flow, while the instant power declined dramatically (5.65%) at the azimuth angle of 180°.

Response of flexible rotor to tower interference: The aeroelastic responses in uniform flow and in tower interference were calculated. The results both showed that the flexible blade generated great deflection deformation under trust force of flow, which reduced the loads of the rotor. In uniform flow, the main shaft torque and flapwise moment of flexible blade root respectively showed reductions of 3.93 and 1.58%, compared to rigid blade assumption. The output power of flexible rotor was 5.03 MW, which showed a reduction of 5.45% than power of rigid blades and it was consistent with the output power given in Jonkman and Butterfield (2009).

The periodic and impulsive load of tower interference forced the blade to vibrate during revolution, as shown in Fig. 7. Figure 8 showed the limiting position of blade vibration in coordinate system 4 and the peak-peak value of the blade tip vibration was 0.191 m.

Figure 9 and 10 showed the blade load during the revolution. Vibration of the blades changed the wind speed seen by blade and then caused the changing of the loads. In the left and right side of azimuth angle of 180 degree zone, the directions of the blade flapwise vibration were opposite; hence the main shaft torque and the flapwise moment of blade root showed an obvious asymmetry. Compared to uniform flow, the maximum response of flexible rotos to tower interference

Fig. 9: Shaft torque of flexible rotor

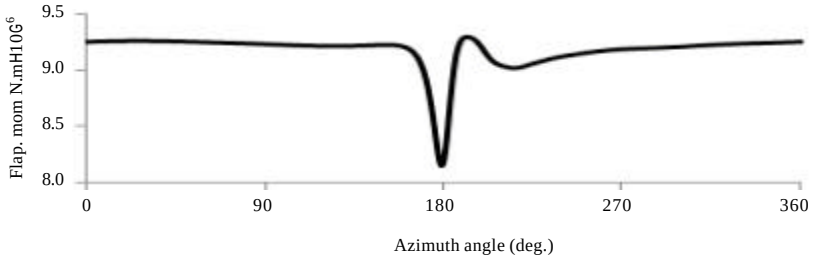

Fig. 10: Flapwise moment of flexible blades

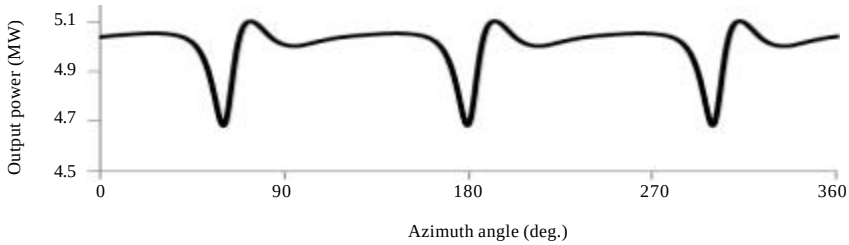

Fig. 11: Output power of flexible rotor

torque and flapwise moment showed apparent increments of 2.86 and 0.58% and the minimum values showed bigger declines of 22.46 and 11.86%. The output power was also affected by tower interference therefore showed an obvious 3P fluctuation of load, as shown in Fig. 11. The average output power showed a very slightly reduction of 1.38% compared to output power in uniform flow, while the instant power declined dramatically (7.49%) at the azimuth angle of 180 degree, which were both bigger than the reduction value under rigid blade assumption.

Responses of rotors with various main axes to tower shadow: In order to reduce the weight of the nacelle therefore pursue higher economic returns, a compact structure with shorter main shaft are often adopted in modern wind turbine. In this paper, based on 5MW-NREL RWT, increasing or decreasing the main shaft length of 10, 20, 30%, respectively and the influence of tower interference on rotors with various shafts were simulated.

During revolution, the blade deflected under the trust force of flow and distances between the tower and blade tip were shown in Table 1. When shortening the main shaft of 20%, the blade tip had been very close to the tower under rated wind speed and it could be predicted that the tower might crash into the tower when the wind speed was bigger than rated wind speed. When shortening the main shaft of 30%, the blade tip had crashed into the tower under rated wind speed.

Figure 12 showed the wind speed seen by blade tip during revolution and Fig. 13 and 14 showed the impulsive loads of rotors with different shaft length. The rotor with the shorter main shaft experienced more severe fluctuation of wind speed and loads. The maximum and minimum fluctuation values were shown in Table 2.

Meanwhile, the output power with shorter shaft fluctuated severely, as shown in Fig. 15. The results of the calculations showed that although the shorter shaft was

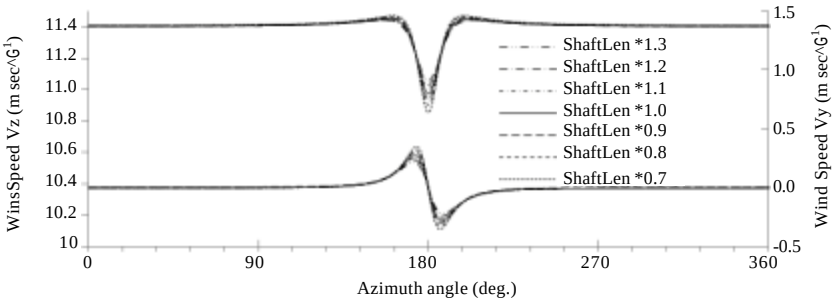

Fig. 12: Speed seen by blade tip with different shaft length

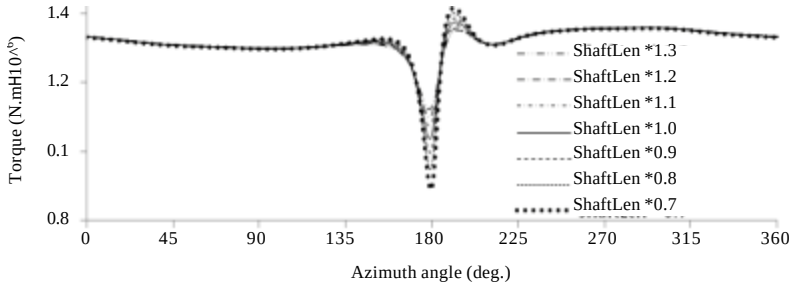

Fig. 13: Torque of main shaft with varying length shaft

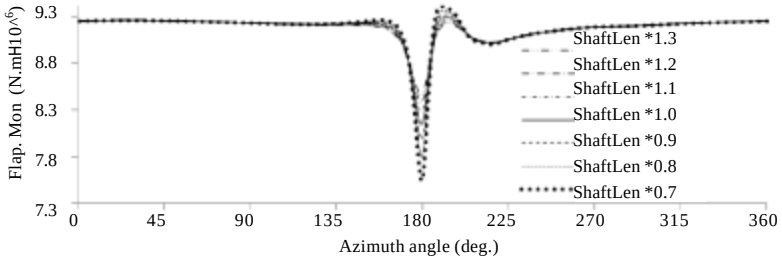

Fig. 14: Flapwise moment of rotor blades with varying main shaft in length during revolution

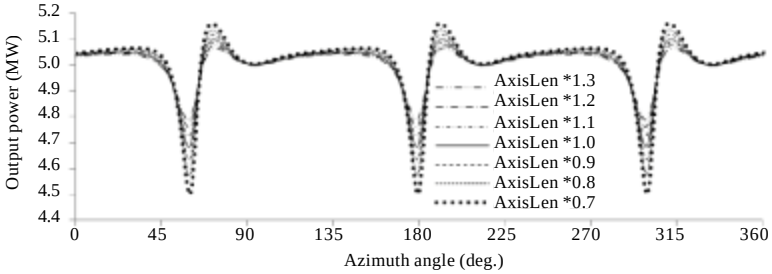

Fig. 15: Output power of rotors with varying main shaft in length during revolution

Table 1: Distance between blade tip and tower

Shaft length	Distance m^{-1}
*1.3	2.67
*1.2	2.18
*1.1	1.68
*1.0	1.18
*0.9	0.68
*0.8	0.18
*0.7	-0.31

Notice that "*1.3" means shortening the main shaft of 30%

Table 2: Fluctuation of load of blades with varying main shaft in length

	Torque		Flap. Mom.	
Shaft Len.	Min.Fluct. (%)	Max.Fluct. (%)	Min.Fluct. (%)	Max.Fluct. (%)
*0.7	6.43	-33.23	1.77	-18.44
*0.8	5.13	-28.80	1.25	-15.76
*0.9	4.08	-25.15	0.82	-13.65
*1.0	3.22	-22.17	0.48	-11.95
*1.1	2.51	-19.67	0.18	-10.57
*1.2	1.96	-17.57	0.09	-9.42
*1.3	1.95	-15.81	0.08	-8.47

benefit to compact the structure of the nacelle therefore decrease the cost, it made the wind turbine experience stronger impulsive load and affected the life of the turbine and the stability of the output power.

CONCLUSION

- Based on potential flow method, the flow field around the tower was calculated. Taking NREL-5MW RWTas example, an aeroelastic model of the wind rotor, combining with quasi-steady BEM method and 1D equivalent beam theory, was established and used to simulate the fluctuation of loads and the output power under rotor-tower interraction
- During tower passage, the blades experienced periodic and impulsive loads and the output power of the rotor showed an obvious 3P fluctuation during tower passage. Although, the average output power showed a very slightly reduction compared to uniform flow, the instant power and th flapwise moment of blade root both fluctuated dramatically at azimuth of 180 degree. To the rotors with rigid blade assumption, the fluctuation value of output power and flapwise moment value were 5.65% and 7.49% respectively, while the fluctuation of the power and flapwise moment to actual flexible rotors were 7.49% and 11.86% respectively, which were bigger than rigid rotors. With increasing size of wind turbine, the blades become more flexible and the impulsive load of rotor-tower interaction cannot be neglected
- To those wind rotors with shorter main shafts, not only the output power but also the loads of the blades fluactuaed more severely, which might shorten the life the wind turbine. When the main shaft was too short, the flexible blades might crash into the tower

ACKNOWLEDGMENTS

This study was supported by the National Natural Science Foundation of China (Grant No. 51105151 and Grant No. 51375183).

REFERENCES

Hansen, M.O.L., 2008. Aerodynamics of Wind Turbines. 2nd Edn., Earthscan, London.

Hansen, M.O.L., J.N. Sorensen, S. Voutsinas, N. Sorensen and H.A. Madsen, 2006. State of the art in wind turbine aerodynamics and aeroelasticity. Prog. Aerospace Sci., 42: 285-330.

Hasegawa, Y., J. Murata and H. Imamura, 2006. Calculation of aerodynamic force on horizontal axis wind turbine rotor exerted by tower effect. European wind energy conference, athens, greece, EWEC 2006. http://proceedings.ewea.org/ewec2006/allfiles2/0179_Ewec2006fullpaper.pdf.

Jonkman, J., S. Butterfield, W. Musial and G. Scott, 2009. Definition of a 5-MW reference wind turbine for offshore system development. Technical Report NREL / TP-500-38060, National Renewable Energy Laboratory, Colorado.

Kong, Y., J. Wang, H. Gu, Z. Wang and D. Xu, 2011. Dynamics modeling of wind speed based on wind shear and tower shadow for wind turbine. Acta Energiae Solaris Sinica, 32: 1237-1244.

Lackner, M.A., N. deVelder and T. Sebastian, 2013. On 2D and 3D potential flow models of upwind wind turbine tower interference. Comput. Fluids, 71: 376-379.

Zahle, F., H.A. Madsen and N.N. Sorensen, 2009. Evaluation of tower shadow effects on various wind turbine concepts. Research in Aeroelasticity EFP-2007-II. Technical Report Riso-R-1698(EN), Riso National Laboratory, Roskilde, pp: 11-29.

Zahle, F., N.N. Sorensen and H.A. Madsen, 2008. The influence of wind shear and tower presence on rotor and w ake aerodynamics using CFD. Research in Aeroelasticity EFP-2007. Technical Report Riso-R-1649(EN), Riso National Laboratory, Roskilde, pp: 17-37.